

Fishing for the FIR Line Deficit in the Local Swimming Hole: Heating and Cooling of Extragalactic ISMs in Early KINGFISH Data

The physical state of interstellar gas and dust is dependent on the processes which heat and cool this medium. The principal mechanisms responsible for the heating and cooling of this gas are thought to be the injection of photoelectrons from dust and far-infrared line emission, respectively. The heating efficiency of the dust is defined as the relative strength of line emission to the heating. In general, as the far-IR dust temperature increases, we see a deficit in the global heating efficiency. To disentangle radiation from an inhomogeneous ISM, we require observations with better spatial resolution. Herschel observations we acquired as part of the KINGFISH program show spatially resolved line emission also exhibits the empirical heating efficiency deficit. However, the ratio of cooling lines and the power emitted by vibrational transitions in PAHs, which supply a significant portion of the photoelectrons, show a constant ratio, except in the in the hottest regions of the ISM. We find that ionized PAHs are responsible for this decrease in heating efficiency in warm regions. We confirm this interpretation based on the ratio of the 7.7 and 11.3 micron PAH features.

Kevin V. Croxall¹, J. D. T. Smith¹, and the KINGFISH Team
¹University of Toledo

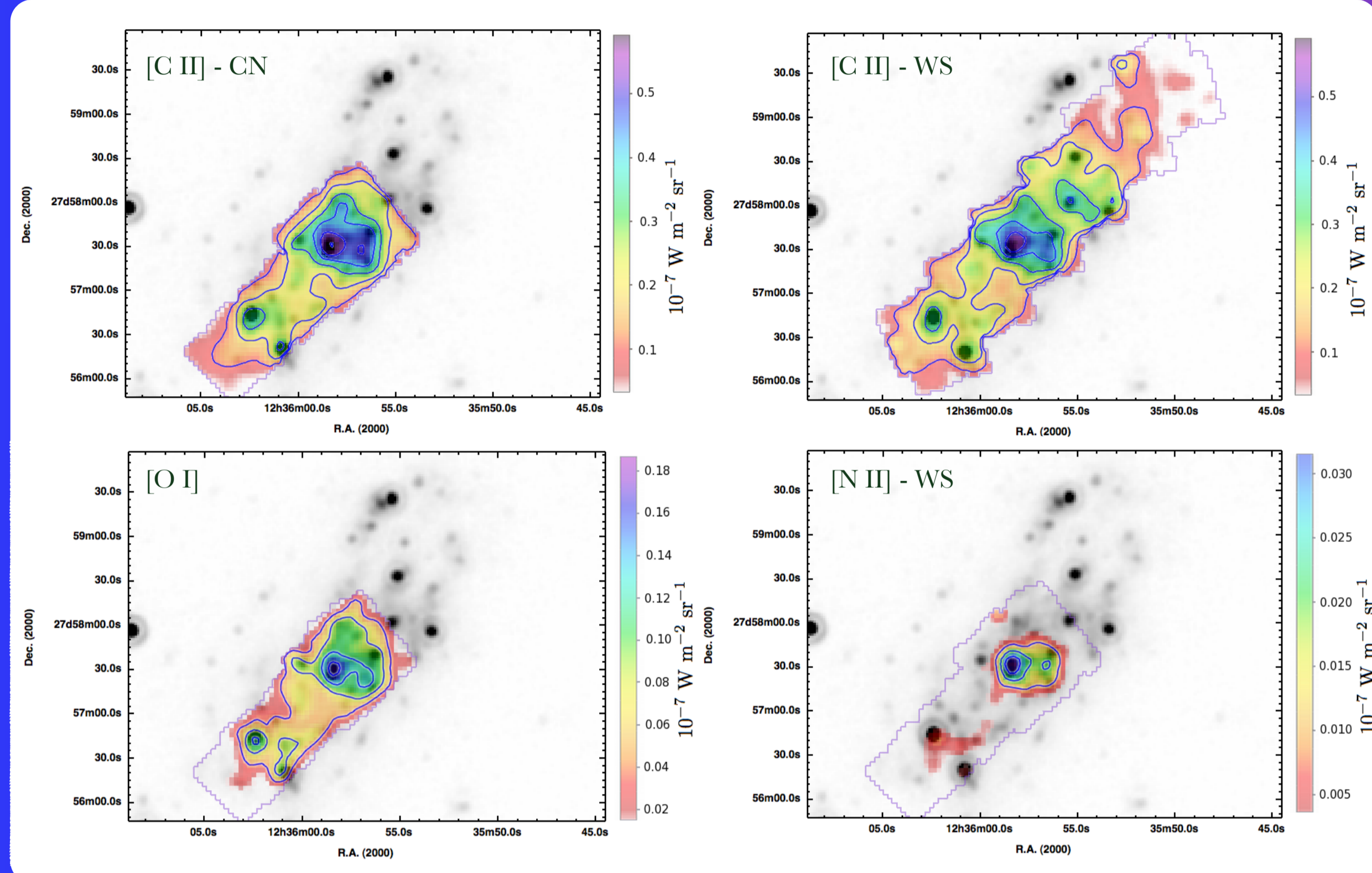


Fig. 1: Contour maps of far-IR fine structure lines in NGC 4559 overlaid on the MIPS 24 μm image. The footprint of the spectral mapping in each line is shown as a faint purple outline. Contours are plotted every 0.10, 0.01, and 0.04 $10^{-7} \text{W m}^{-2} \text{sr}^{-1}$ for [C II], [N II], and [O I]. Line maps are clipped below a S/N of 2σ .

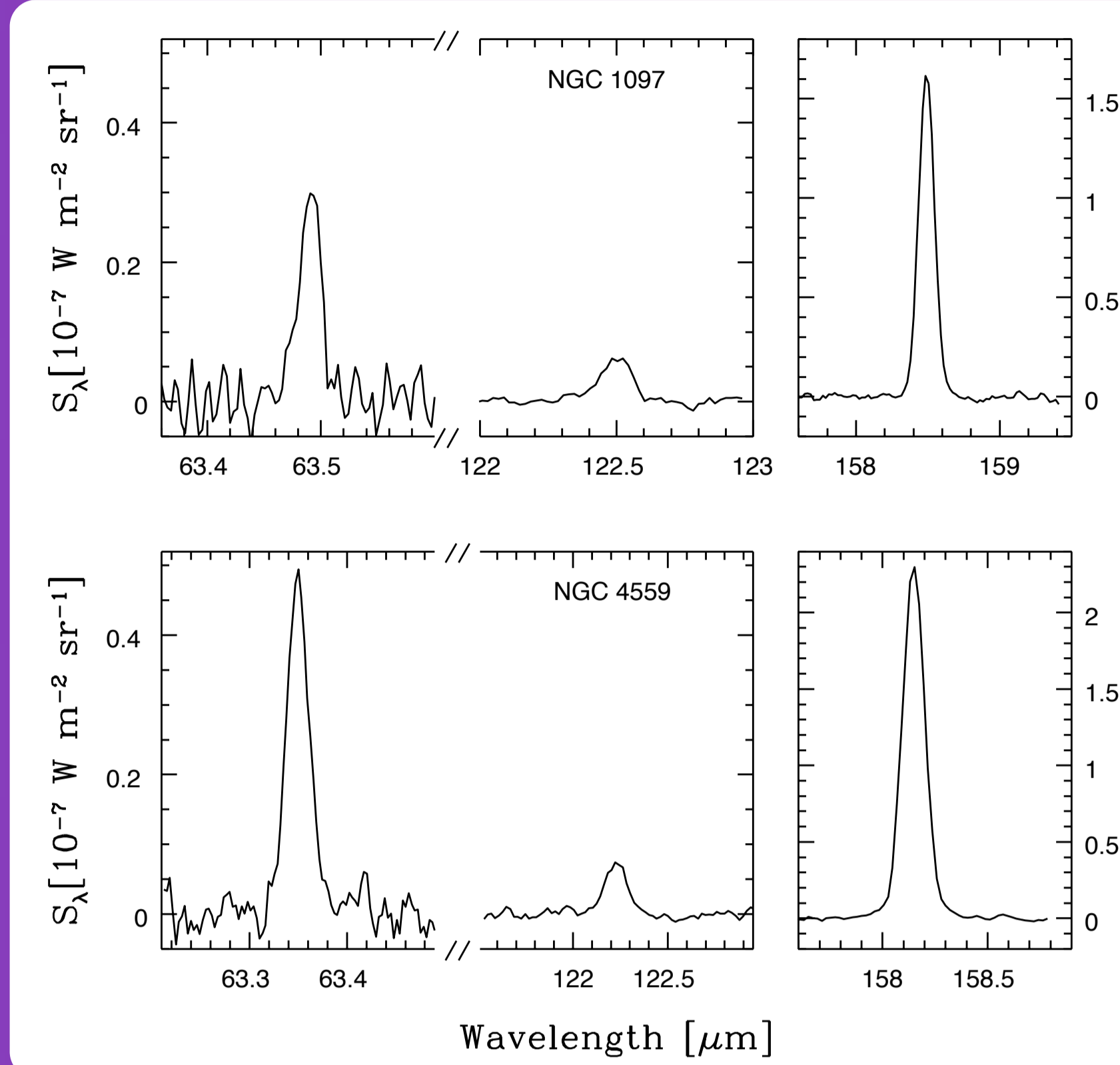


Fig. 2: Representative spectra from regions with [N II] 122 μm detections in diffuse regions of NGC 1097 (top) and the nuclear region of NGC 4559 (bottom). The [O I] 63 μm line and the [N II] 122 μm line are plotted on the same scale.

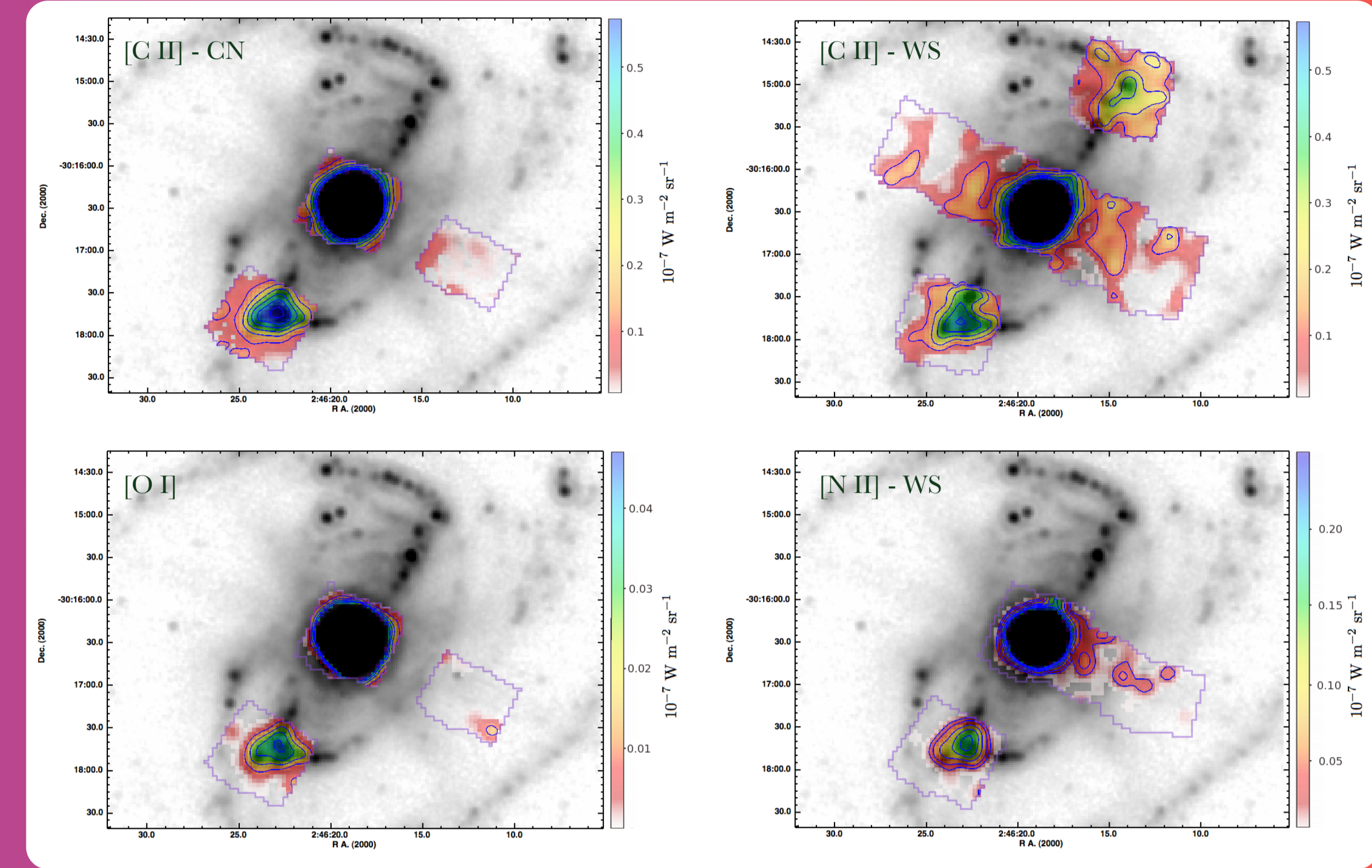


Fig. 3: Contour maps of far-IR fine structure lines in NGC 1097 overlaid on the MIPS 24 μm image. The footprint of the spectral mapping in each line is shown as a faint purple outline. Contours are plotted every 0.10, 0.6, and 0.01 $10^{-7} \text{W m}^{-2} \text{sr}^{-1}$ for [C II], [N II], and [O I]. Line maps are clipped below a S/N of 2σ .

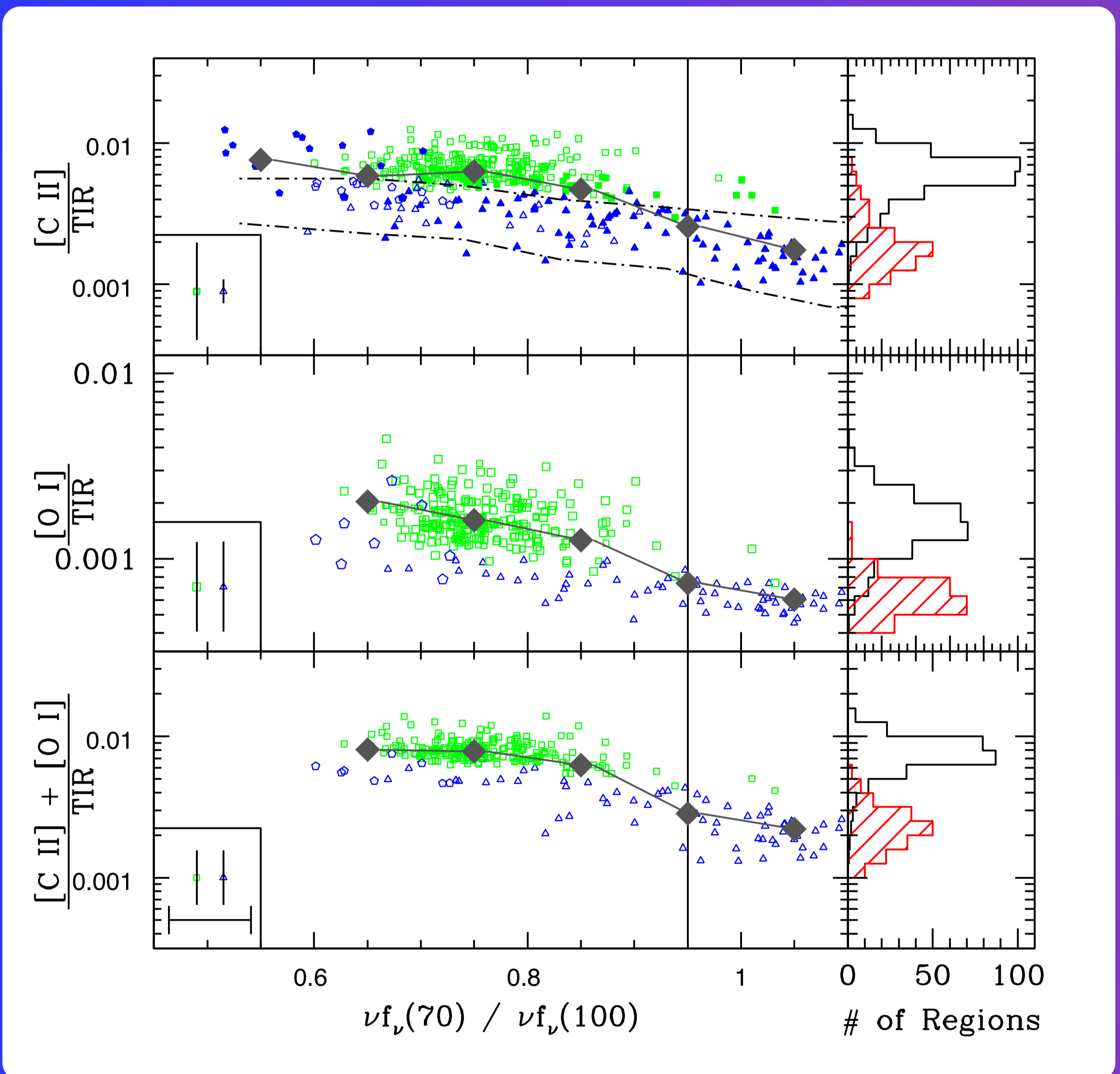


Fig. 4: Top: [C II] 158 μm / TIR plotted as a function of the far infrared color, $\nu_{\text{fv}}(70)/\nu_{\text{fv}}(100)$. Middle: [O I] 63 μm / TIR plotted as a function of the far infrared color, $\nu_{\text{fv}}(70)/\nu_{\text{fv}}(100)$. Bottom: ([C II] 158 μm + [O I] 63 μm) / TIR plotted as a function of the far infrared color, $\nu_{\text{fv}}(70)/\nu_{\text{fv}}(100)$. Even when accounting for the oxygen emission from denser regions, the photoelectric heating efficiency decreases with increasingly intense radiation. Regions in NGC 1097 are plotted as blue triangles (regions in the strip) and pentagons (regions from the extra-nuclear regions) whereas regions from NGC 4559 are plotted as green squares. The large grey diamonds show the trend when data are binned. Histograms show the distribution of heating intensity for regions with gas warmer (red, scaled up by a factor of 5) and cooler (black) than $\nu_{\text{fv}}(70)/\nu_{\text{fv}}(100) = 0.95$. [N II], and [O I]. Line maps are clipped below a S/N of 2σ .

- KINGFISH is an open-time Herschel key program investigating nearby galaxies.
- Observations are matched to those of SINGS to acquire a full suite of IR diagnostics.
- We present an analysis of the heating and cooling in the first two KINGFISH galaxies observed, NGC 1097 and NGC 4559.
- 10'' extraction apertures are tiled along KINGFISH observations.
- The scatter in $([\text{C II}] + [\text{O I}])/\text{PAH}$ is reduced compared to $([\text{C II}] + [\text{O I}])/\text{TIR}$ (Fig. 4 & 5).
- Both [C II] and [O I] exhibit line deficits relative to both TIR and PAH emission.
- Heating efficiency (PE) traced by $([\text{C II}] + [\text{O I}])/\text{TIR}$, decreases as dust temperature rises (Fig. 4).
- In contrast, $([\text{C II}] + [\text{O I}])/\text{PAH}$ is flat as the temperature of the dust increases, up to $\nu_{\text{fv}}(70 \mu\text{m})/\nu_{\text{fv}}(100 \mu\text{m}) \sim 0.95$ (Figure 5).
- In warm regions, $\nu_{\text{fv}}(70 \mu\text{m})/\nu_{\text{fv}}(100 \mu\text{m}) > 0.95$, there is a drop in the ratio of line to PAH.

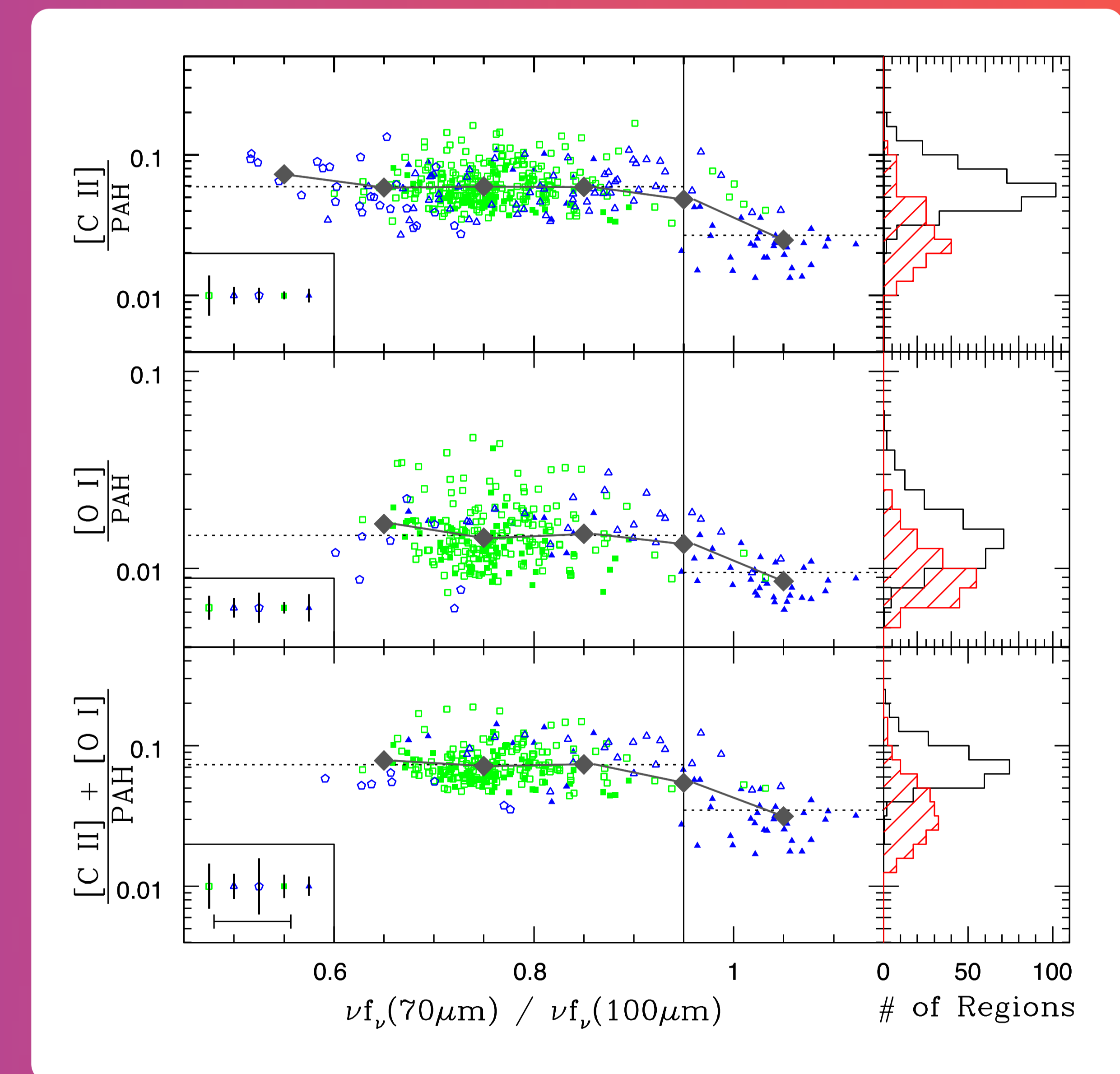


Fig. 5: Top: [C II] 158 μm / PAH plotted as a function of the far infrared color, $\nu_{\text{fv}}(70)/\nu_{\text{fv}}(100)$. Middle: [O I] 63 μm / PAH plotted as a function of the far infrared color, $\nu_{\text{fv}}(70)/\nu_{\text{fv}}(100)$. Bottom: ([C II] 158 μm + [O I] 63 μm) / PAH plotted as a function of the far infrared color, $\nu_{\text{fv}}(70)/\nu_{\text{fv}}(100)$. Regions in NGC 1097 are plotted as blue triangles and pentagons whereas regions from NGC 4559 are plotted as green squares. Filled points indicate regions wherein PAH was measured in the full IRS spectrum, while open points denote estimates of PAH from Equations 5 (triangles and squares) and 6 (pentagons). The large grey diamonds show the trend when data are binned. Histograms show the distribution of heating intensity for regions with gas warmer (red, scaled up by a factor of 5) and cooler (black) than $\nu_{\text{fv}}(70)/\nu_{\text{fv}}(100) = 0.95$. [N II], and [O I]. Line maps are clipped below a S/N of 2σ .

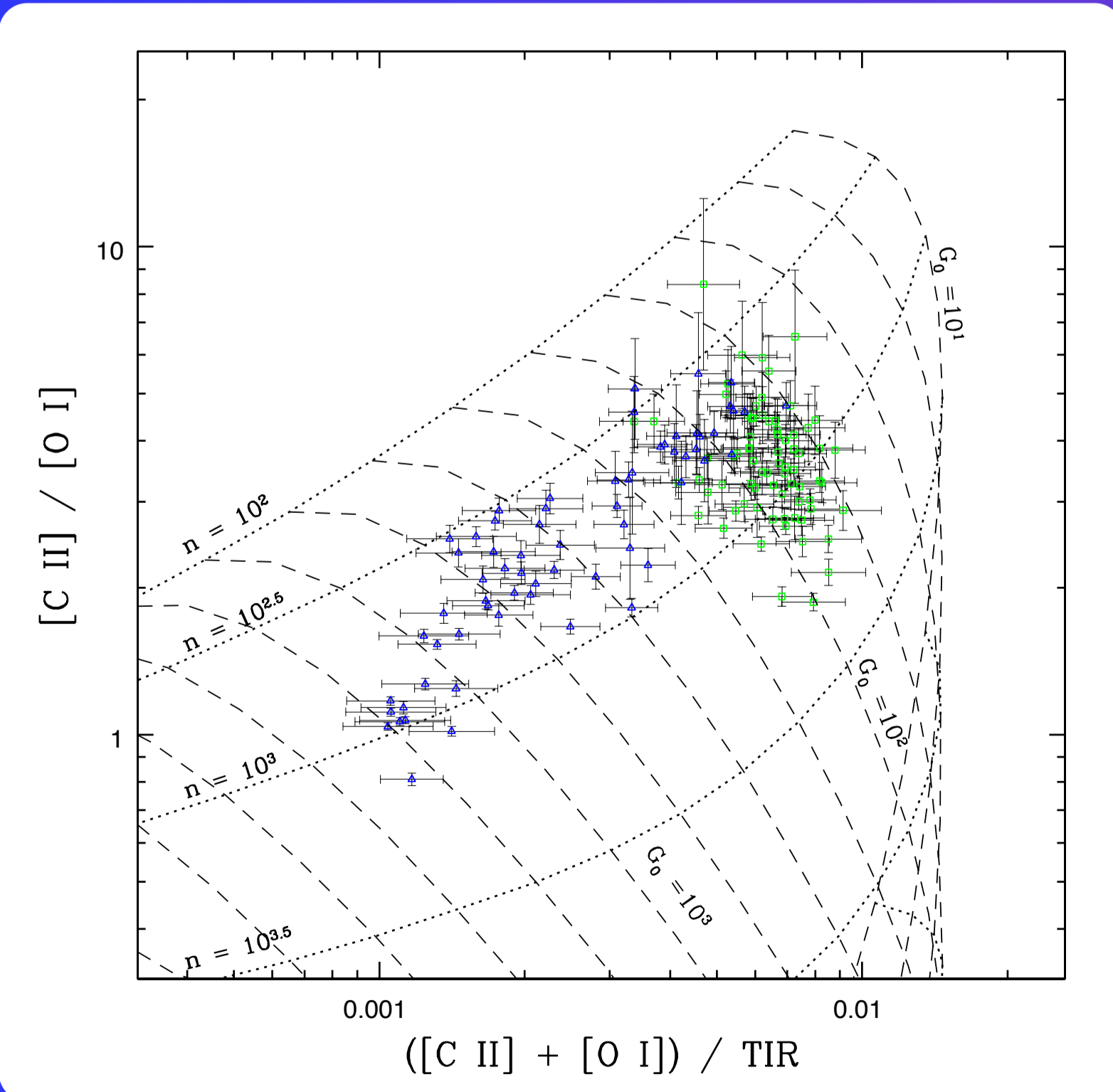


Fig. 6: [C II] 158 μm / [O I] 63 μm plotted against $([\text{C II}] 158 \mu\text{m} + [\text{O I}] 63 \mu\text{m})/\text{TIR}$ for NGC 1097 (blue triangles) and NGC 4559 (green squares). A grid of G_0 and D_{H} , as determined from the PDR models of Kaufman et al. (2006) are overplotted. Error bars do not include uncertainty in the correction for diffuse [C II] emission.

Many explanations have been proposed to explain the deficit observed in the observed heating efficiency. In regions of NGC 1097 and NGC 4559 we find:

- A_{v} along the line of sight is insufficient to cause self absorption of [C II] and [O I]
- Star formation is on going supplying ionizing radiation in warm regions
- Deficits are not observed in the [N II] or [Si II] lines, as would be expected if dusty ionization regions caused the deficit.
- No regions observed are dense enough that saturation of [C II] emission will occur (see Fig. 6).
- If [C II] did saturate, cooling by [O I] should compensate in dense gas, this is not the case
- The distribution of the 7.7/11.3 μm PAH band strength ratio is different below and above $\nu_{\text{fv}}(70 \mu\text{m})/\nu_{\text{fv}}(100 \mu\text{m}) \approx 0.95$ (see Figure 7).
- The far-IR line deficit in these galaxies is consistent with warm, less efficiently heated gas being populated by ionized PAHs.

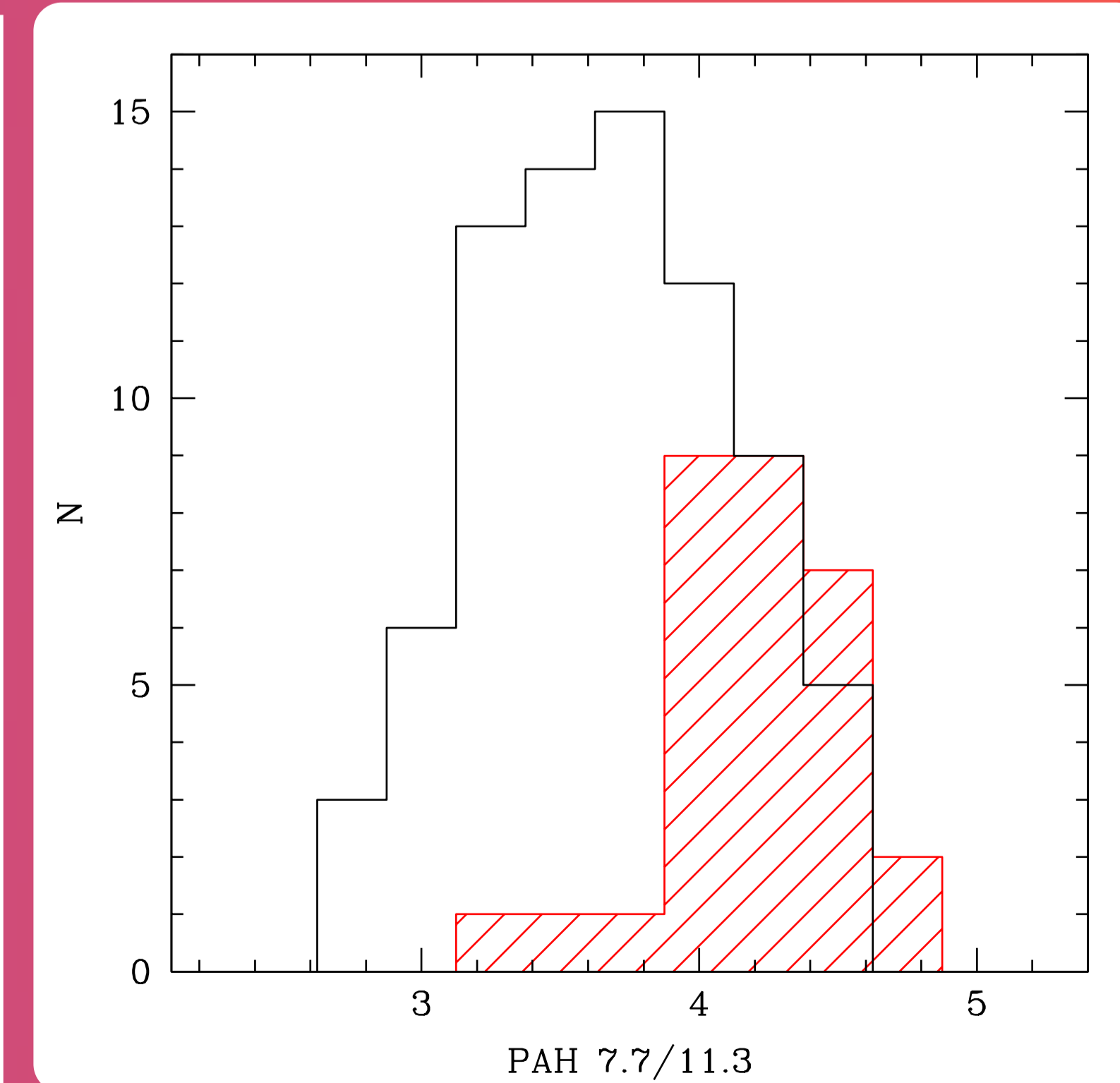


Fig. 7: Histogram of the PAH 7.7 / 11.3 μm ratio. Regions for which $\nu_{\text{fv}}(70)/\nu_{\text{fv}}(100) < 0.95$ are indicated with the black histogram, whereas regions with $\nu_{\text{fv}}(70)/\nu_{\text{fv}}(100) > 0.95$ are indicated with the red histogram. An increase in this ratio in regions typified by warm dust is indicative of an increase in PAH ionization.

